LECTURE 11. INTRODUCTION TO THE AICON PROGRAM

I will give you a detailed introduction about the models implemented in AICON. As I talked in the last section, all electronic transport properties can be expressed by a series of generalized transport coefficients. The main difficulty is how to calculate electronic relaxation time \tau.

Considering the scattering processes an electron should have been through, the total relaxation time, according to Matthiessen's rule, should include scattering effect from acoustic phonon, optical phonon, impurity ions, grain boundary, dislocation, etc. In AICON, we only consider the first three scattering.

Electronic relaxation time, according to Matthiessen's rule:

$$\frac{1}{\tau} = \frac{1}{\tau_{aco}} + \frac{1}{\tau_{opt}} + \frac{1}{\tau_{imp}} + \frac{1}{\tau_{BD}} + \dots$$

Acoustic phonon scattering is the most important scattering process in the interested temperature and carrier concentration range. which can be described by deformation potential theory proposed by Bardeen in1950s, the basic assumptions behind this theory are the studied objects are isotropic crystal, all the scattering process are elastic, the material is under nondegenerate state(pure or very low doping), the relationship between energy and wave vector is parabolic, and effective mass of carrier equals to mass of electron, which means constant energy surface is sphere. Bardeen's method was proposed for calculating mobility of nonpolar semiconductors, such as Si. The theory need to be extended in order to apply to wider range of materials, for example, usually the materials are in degenerate states because of the doping, the energy band is not strictly parabolic, especially near the boundary of the Brillouin zone, the constant energy surface are usually not sphere, a ellipsoidal constant energy surface should be more common.

- acoustic phonon scattering

τ_{aco} can be described by deformation potential theory proposed by Bardeen [2]

- Isotropic crystal
- Elastic scattering
- Nondegenerate → Degenerate
- Energy band is parabolic → Nonparabolicity
- Effective mass of carrier equals to mass of electron (constant energy surface is sphere) → Ellipsoidal constant energy surface

[2] Bardeen J, Shockley W., Physical review, 1950, 80(1): 72.

At the first step, we need a model to describe the band energy-wave vector relationship, which usually uses the Kane band model. In this model, for lowest conduction band or highest valence band, the energy dispersion law can be expressed as, here vertical and parallel symbol means transverse and longitudinal direction of ellipsoidal energy surface, epsilon is the band energy and epsilon g is the band gap. The part in brace indicating the nonparabolicity. Then energy dependence of effective mass can be expressed as, the density of states is , here md is so called density of states effective mass, with N represent band degeneracy due to the symmetry. Based on the above approximation,

Modified Kane band model within the framework of **k-p** theory, [3]

The energy dispersion law

$$\frac{\hbar^2 k_\perp^2}{m_{\perp 0}^*} + \frac{\hbar^2 k_\parallel^2}{2m_{\parallel 0}^*} = \xi\left(1 + \frac{\xi}{\xi_g}\right)$$

The energy dependency of effective mass

$$m_i^* = m_{i0}^*\left(1 + \frac{2\xi}{\xi_g}\right) = m_{i0}^*\left(1 + 2\beta z\right)$$

The density of states

$$\rho = \frac{2^{1/2} m_d^{3/2}}{\pi^2 \hbar^3} \xi^{1/2}\left(1 + \frac{\xi}{\xi_g}\right)^{1/2}\left(1 + \frac{2\xi}{\xi_g}\right) \quad \text{with} \quad m_d^* = N^{2/3}\left(m_\parallel^* m_\perp^{*2}\right)^{1/3}$$

[3] Y. I. Ravich, *et al.*, Semiconducting Lead Chalcogenides, Plenum Press, New York, 1970

The deformation potential theory can be extended and the scattering rate of electron-acoustic phonons is. Here E1 is the deformation potential constant, cl is direction averaged elastic constant. The factor outside the bracket is the same as the formula proposed by Bardeen, the factor in the bracket as function of two quantities z and Beta describes the energy dependence of the squared coupling matrix element. It is a correction to the parabolic band model.

Formula for electron-acoustic phonon scattering:

$$\frac{1}{\tau_{aco}(z)} = C|M|^2 \rho = \frac{\pi k_0 T \rho(z) E_1^2}{\hbar c_l N}\left[1 - \frac{8\beta\left(z+\beta z^2\right)}{3(1+2\beta z)^2}\right]$$

Here,

$$z = \frac{\xi}{k_B T} \qquad \beta = \frac{k_B T}{\xi_g}$$

The factor in bracket as function of two quantities z and β describes the energy dependence of the squared coupling matrix element.

In a polar crystal, at some temperatures the polar scattering by long-wavelength longitudinal optical phonons shows approximately the same temperature dependence as the acoustic phonon scattering. It has the form like this, Where ε∞ and ε0 are the high frequency and static dielectric constants. The tao optic is also a function of band energy and temperature. The factor in braces describes the energy dependence of the squared matrix element and screening effect (δ) from free carriers.

In real applications, there is always doping in semiconductors, so we also need to consider scattering from impurity.

- polar optical phonon scattering

$$\frac{1}{\tau_{\text{opt}}(z)}=\frac{2^{1/2}k_0Te^2m_{d1}^{*1/2}\left(\varepsilon_\infty^{-1}-\varepsilon_0^{-1}\right)}{\hbar^2\left(zk_0T\right)^{1/2}}\frac{1+2\beta z}{\left(1+\beta z\right)^{1/2}}$$
$$\times\left\{\left[1-\delta\ln\left(1+\frac{1}{\delta}\right)\right]-\frac{2\beta\left(z+\beta z^2\right)}{\left(1+2\beta z\right)^2}\left[1-2\delta+2\delta^2\ln\left(1+\frac{1}{\delta}\right)\right]\right\}$$

The factor in braces describes the energy dependence of the squared matrix element and screening effect (δ).

- ionized impurity scattering in highly degenerate samples

$$\frac{1}{\tau_{\text{imp}}}=\frac{2e^4Nm_{d1}^*\left(1+2\zeta/\xi_g\right)\Phi\left(\delta_0\right)}{3\pi\varepsilon_0^2\hbar^3}$$

Here $\Phi(\delta)$ describes the screen effect from carriers:

$$\Phi\left(\delta_0\right)=\ln\left(1+\delta_0^{-1}\right)-\left(1+\delta_0\right)^{-1}$$

A short summary, based on the formula I listed previously, electronic transport properties can be easily calculated, all the parameters we need to know are just these six parameters, and they all can be calculated by first principle method easily.

The key parameters involved in scattering rate, which need to be calculate by first-principles method:

- ❑ Effective mass
- ❑ Elastic constant
- ❑ Band gap
- ❑ Band degeneracy
- ❑ Deformation potential constant
- ❑ Dielectric constant

For lattice thermal conductivity calculation, we adopted the Debye Callaway model. The original Callaway model based on these four assumptions: and only consider longitudinal acoustic phonon

Debye-Callaway model

The original Callaway model based on four assumptions:

- only acoustic phonons account for lattice thermal conductivity
- the crystal vibration spectrum is isotropic and dispersion-free
- four scattering mechanisms are considered, including point impurities (isotopes disorder), normal three-phonon processes, Umklapp processes and boundary scattering
- phonon scattering processes can be represented by frequency-dependent relaxation times

Later, the model was developed and Morelli gave specific formulas for kappa of three acoustic phonon branches, the total kappa L is the sum of their contribution. Each of them includes two parts, and each part can be calculated as this. Many parameters here are just constants or can be easily obtained. There are only three parameters need to be carefully calculated. They are the gruneisen parameter gamma, phonon velocity v, and Debye temperature of each acoustic phonon branch theta. Before, these parameters were obtained from experimental measurement or fitted from experimental data. But now, these parameters can be calculated using density function theory directly.

According to Morelli[4]

$$\kappa = \kappa_{LA} + 2\kappa_{TA}$$

$$\kappa_i = \kappa_{i1} + \kappa_{i2} \quad i \text{ denoting } LA, TA$$

$$\kappa_{i1} = \frac{1}{3} C_i T^3 \int_0^{\theta_i/T} \frac{\tau_C^i(x) x^4 e^x}{\left(e^x - 1\right)^2} dx \qquad \kappa_{i2} = \frac{1}{3} C_i T^3 \frac{\left[\int_0^{\theta_i/T} \frac{\tau_C^i(x) x^4 e^x}{\left(e^x - 1\right)^2} dx\right]^2}{\int_0^{\theta_i/T} \frac{\tau_C^i(x) x^4 e^x}{\tau_N^i(x)\tau_R^i(x)\left(e^x - 1\right)^2} dx}$$

$$C_i = k_B^4 / 2\pi^2 \hbar^3 v_i \quad x = \hbar\omega / k_B T \quad \left(\tau_C^i\right)^{-1} = \left(\tau_N^i\right)^{-1} + \left(\tau_R^i\right)^{-1} \quad \left(\tau_R^i\right)^{-1} = \left(\tau_U^i\right)^{-1} + \left(\tau_I^i\right)^{-1} + \left(\tau_B^i\right)^{-1}$$

$$\left[\tau_N^L(x)\right]^{-1} = \frac{k_B^3 \gamma_L^2 V}{M\hbar^2 v_L^5}\left(\frac{k_B}{\hbar}\right)^2 x^2 T^5 \quad \left[\tau_N^T(x)\right]^{-1} = \frac{k_B^4 \gamma_T^2 V}{M\hbar^3 v_T^5}\left(\frac{k_B}{\hbar}\right) x T^5 \quad \left[\tau_U^i(x)\right]^{-1} = \frac{\hbar\gamma_i^2}{M v_i^2 \theta_i}\left(\frac{k_B}{\hbar}\right)^2 x^2 T^3 e^{-\theta_i/3T}$$

[4] Morelli, D. T., J. P. Heremans, and G. A. Slack. *Physical Review B* **66**.19 (2002): 195304.

Furthermore, I improved the model by adding the contributions from optical phonon branches. Because they are important at high temperatures or in compounds with complex structure, which means the primitive cell contains many atoms. The updated formula is this. Using a weight average method, I compress all optical phonon branches into one pseudo optical branch and in its formula I used Einstein model instead of usual Debye model to calculate its specific heat, which should be more accurate for optical phonons. Until now I have talked about the model for calculating electronic transport properties and phonon transport properties respectively. How good are these models?

Contribution from optical phonons can be important, for example, at high temperature, or compounds with complex structure.

$$\kappa = \kappa_{\mathrm{LA}} + \kappa_{\mathrm{TA}} + \kappa_{\mathrm{TA'}} + \kappa_{\mathrm{O}}$$

with

$$\kappa_{\mathrm{O}} = \frac{1}{3} C_V v^2 \tau = \frac{1}{3}(3p-3)\frac{N}{V} k_{\mathrm{B}} f_{\mathrm{E}}\left(\frac{\Theta_E}{T}\right) v_{\mathrm{O}}^2 \tau_C^{\mathrm{O}} \left[1 + \frac{\tau_R^{\mathrm{O}}}{\tau_N^{\mathrm{O}}}\right]$$

$$f_{\mathrm{E}}(x) = x^2 \frac{e^x}{\left(e^x - 1\right)^2}$$

The electronic transport model was tested for carrier mobility and seebeck coefficient, respectively. This table shows the testing set for carrier mobility. including both n type and p type. The temperature and carrier concentration correspond to experimental measurement conditions. The calculations were run at the same condition, then the computed results and experimental results were compared to see how agreement it is.

Mobility test

Materials	Doping	*T* (K)	*n* (cm^{-3})	Materials	Doping	*T* (K)	*n* (cm^{-3})
$CuAlO_2$	p-type	300-430	1.3×10^{17}	PbTe	n-type	300-600	1.8×10^{19}
CdS	n-type	100-400	5.0×10^{15}	PbTe	p-type	300-800	1.4×10^{20}
CdSe	n-type	200-1200	1.0×10^{17}	SiC	n-type	100-900	4.0×10^{15}
CdTe	n-type	200-1200	1.0×10^{15}	SnO_2	n-type	300-700	1.0×10^{17}
GaAs	n-type	300-1000	3.0×10^{13}	SnSe	p-type	300-900	3.3×10^{17}
GaAs	p-type	300-600	6.4×10^{19}	ZnO	n-type	300-1000	8.2×10^{16}
GaN	n-type	150-500	3.0×10^{16}	ZnS	n-type	300-650	1.0×10^{16}
GaP	n-type	100-500	3.0×10^{16}	ZnSe	n-type	200-1300	1.0×10^{15}
InP	n-type	100-700	1.5×10^{16}	Bi_2Te_3	n-type	300-500	3.3×10^{19}
PbS	n-type	300-900	3.6×10^{17}	Bi_2Te_3	p-type	200-500	1.1×10^{19}

This picture shows the results of mobility test. Generally, The calculated values agree reasonably with experiment across all materials, covering several orders of magnitude from 3 cm2/Vs for p-type CuAlO2 at 300 K to 1×10^4 cm2/Vs for n-type GaAs at 300 K. Most examples show a bit large difference at lower temperature, while the difference becomes smaller at higher temperature.

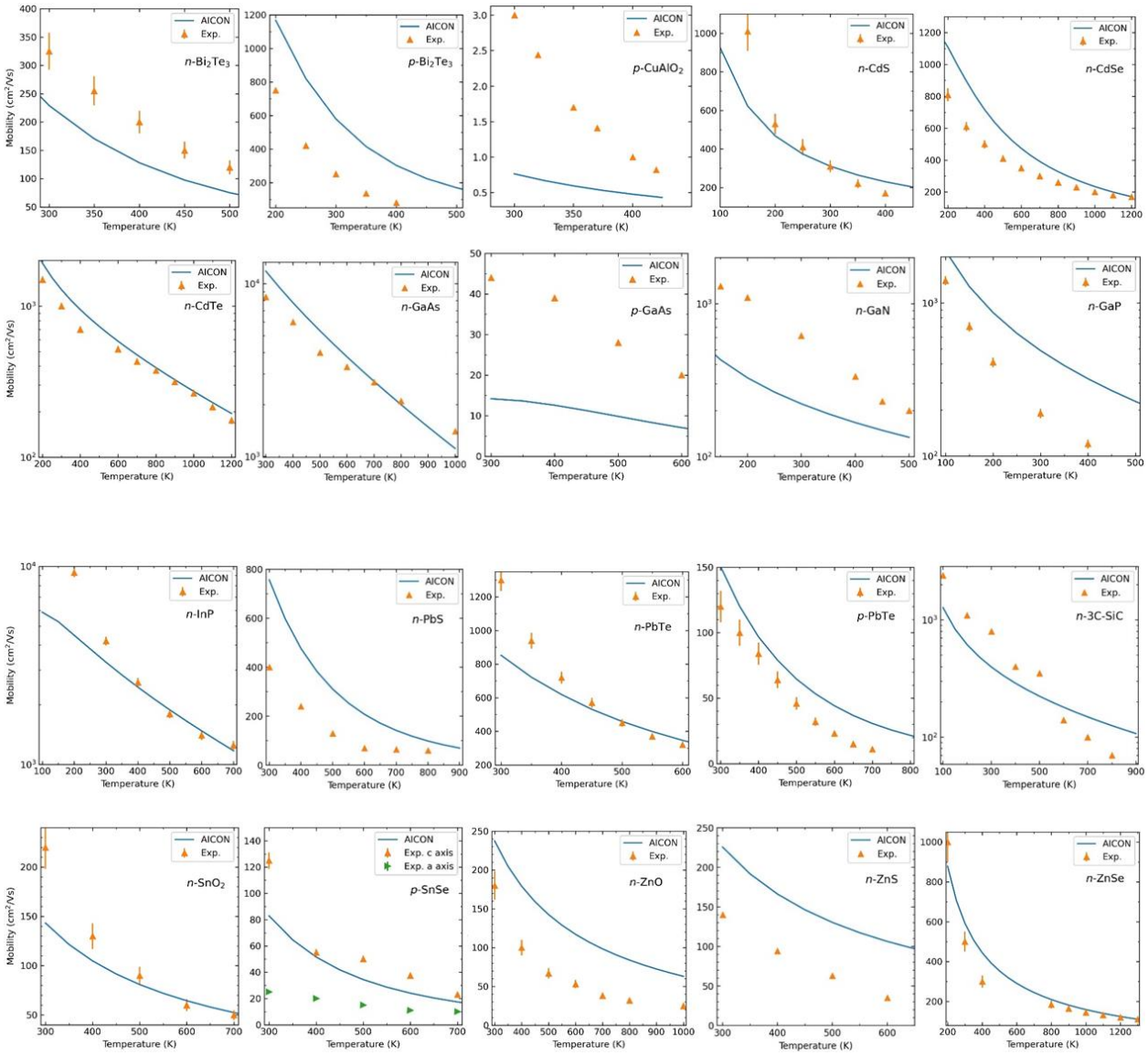

This table lists the compounds used for testing seebeck coefficient and their experimental conditions.

Seebeck coefficient test

Materials	Doping	T (K)	n (cm^{-3})
CdS	n-type	100-300	2.8×10^{15}
GaAs	n-type	400-750	3.5×10^{17}
GaAs	p-type	300-700	6.4×10^{19}
GaN	n-type	100-300	1.3×10^{19}
InP	n-type	150-700	2.1×10^{17}
PbS	n-type	300-800	2.5×10^{19}
PbTe	n-type	300-800	1.8×10^{19}
PbTe	p-type	300-800	1.4×10^{20}
SnO_2	n-type	300-800	8.2×10^{18}
SnSe	p-type	300-900	3.3×10^{17}
ZnO	n-type	200-1000	5.2×10^{17}

This page shows the calculated Seebeck coefficients against those obtained experimentally. Again, reasonable agreement with experiment is achieved for these samples. The largest difference comes from GaAs, both n-type and p-type. The experimental values are almost two times of those of calculation.

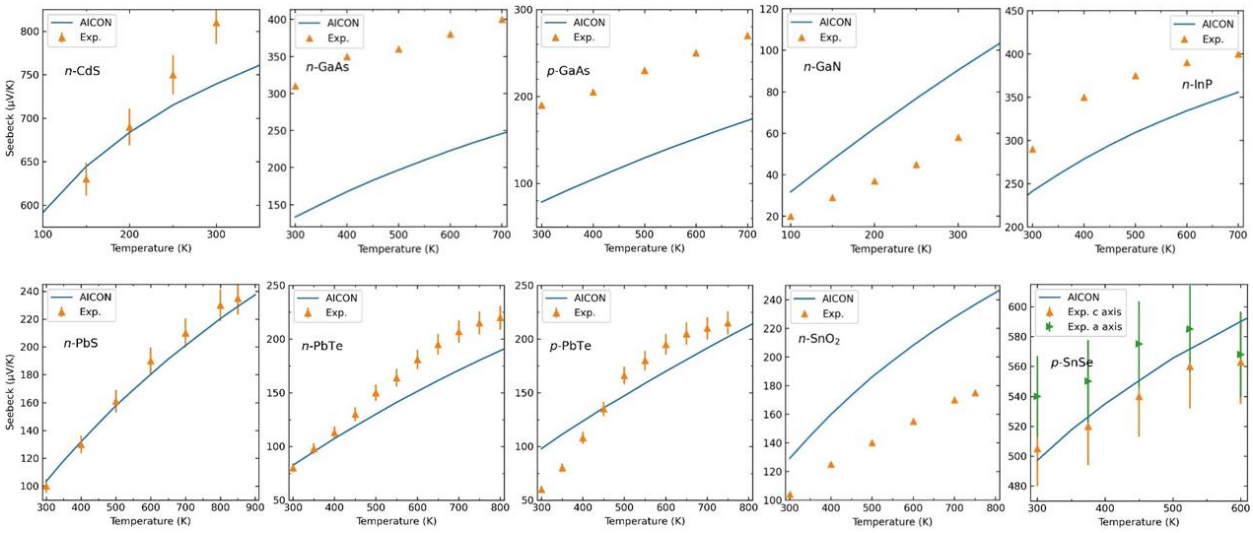

The lattice thermal conductivity model was tested on a set of 27 well known inorganic materials. For this testing set, I try to include as many as elements thus make the set as diverse as possible. Meanwhile, the kappa values of the testing materials should cover a large range. This table shows the compounds and experimental and calculated values at 300 K. The root mean square relative

deviation, which is a measure of the quantitative difference between two variables, is 30%, which means averagely, the calculated values are different 30% with respect to experimental values.

Calculated and experimental lattice thermal conductivity of testing compounds at 300 K
unit: $W \cdot m^{-1} \cdot K^{-1}$

Formula	κ_{exp}	κ_{cal}	Formula	κ_{exp}	κ_{cal}
C(Dia)	2200	2325.41	NaI	1.8	1.92
Si	141	135.83	PbS	2.9	2.69
AgCl	1	0.57	RbBr	3.8	1.55
BaO	2.3	4.27	RbI	2.3	0.99
CaO	27	29.79	SrO	12	14.98
KBr	3.4	2.41	CdF_2	4.3	2.25
KCl	7.1	2.42	$SrCl_2$	2.3	2.84
KI	2.6	1.29	Mg_2Si	12.14	13.47
LiF	17.6	16.48	Mg_2Ge	15.7	20.47
LiH	15	33.28	Mg_2Sn	11.1	9.67
MgO	60	65.42	CaF_2	9.76	7.21
NaBr	2.8	2.02	CeO_2	10.8	7.98
NaCl	7.1	4.04	ZnO	37.5	18.76
NaF	16.5	12.97			

In this figure, the x axis represents calculated values, the y axis represents the experimental values, generally, the calculated values and experimental values correspond quite well. The Pearson correlation coefficient, which is a measure of linear correlation between two variables, is 0.9999, indicating very strong correlation. Another index I use is root mean square relative deviation, which is a measure of the quantitative difference between two variables, is 50.13%, which means averagely, the calculated values are different 50% with respect to experimental values. From the figure, we can see the model is good for compounds with medium and large lattice thermal conductivity, while for those with small kappa, especially those with kappa less than 3, our model tends to underestimate the values. This is a place that needs to be improved in the future.

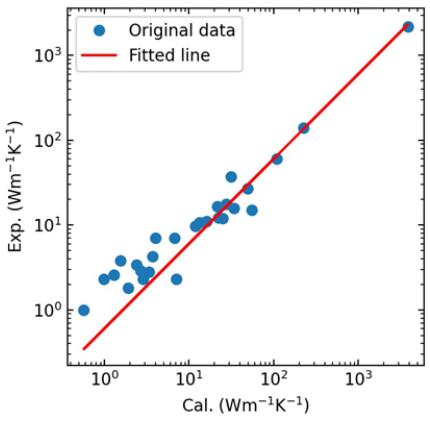

❑ Pearson correlation coefficient *r*:

$$r = \frac{\sum_i (X_i - \bar{X})(Y_i - \bar{Y})}{\sqrt{\sum_i (X_i - \bar{X})^2}\sqrt{\sum_i (Y_i - \bar{Y})^2}}$$

❑ root-mean-square relative deviation (RMSrD):

$$\mathrm{RMSrD} = \sqrt{\frac{\sum_i \left(\frac{X_i - Y_i}{X_i}\right)^2}{N_{\{X,Y\}} - 1}}$$

	K_{cal}	K_{cal_cor}
r	0.9999	0.9999
RMSrD	85.77%	50.13%

$K_{cal\_cor} = W \times K_{cal}$ ($W = 0.6037$)

Next, I will introduce an example of using AICON to screen thermoelectric materials. I extracted the structures from materials project, The selective standards are follows: S(sulfur), Se(selenium), Te(tellurium) as the only sublattice, the bandgap should less than 1.2 eV, because good thermoelectric materials are usually narrow gap semiconductor, energy above convexhull should be less than 0.1 eV, so the structures obtained are experimentally available. Also symmetry is considered from high symmetry cubic structures to low symmetry ones.

Objects: Chalcogenides

Database: Materials Project

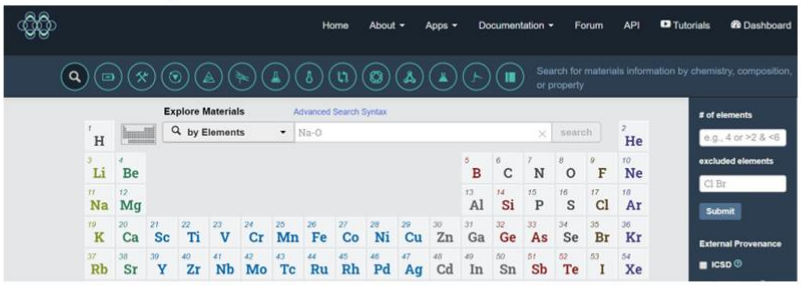

Standards:

Elements	Band gap	E_above_convexhull	Symmetry
S, Se, Te anions	0 < $\mathcal{E}$g < 1.2 eV	<= 0.1 eV	Cubic (Tetragonal, Orthorhombic, Hexagonal, …)

Based on the above selection rules, I have screened 463 structures, and there are 361 structures that finished the whole process of electronic transport properties calculation. These two pictures show a summary of the results. The left for n type,

the right for p type. The y axis represents the maximum power factor one compound can reach in the temperature range of 300 K to 1000 K, the x axis represents the carrier concentration corresponding to the maximum value. The red line means the maximum power factor equal to 10 microwatt per centimeter per Kelvin square. Above this line, the compounds are thought as promising and go forward to calculating their lattice thermal conductivity and figure of merit. Some representative compounds are marked in the picture. Among these compounds, six of them, PbTe, PbS, PbSe, GeTe, SnTe, SnSe are already well-known thermoelectric materials and have high power factor values according to our calculation, which validates our methods.

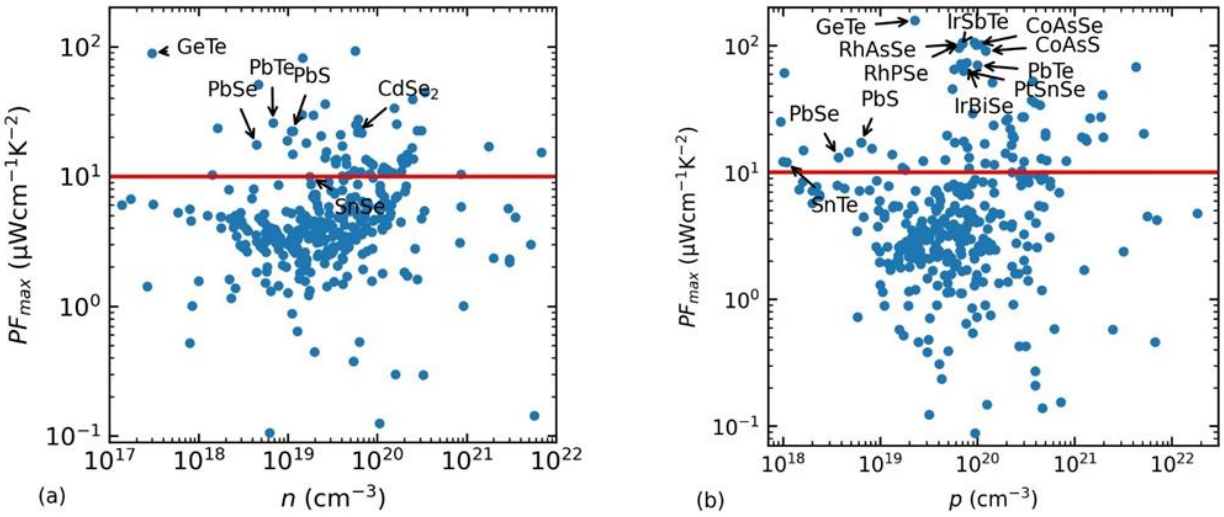

Figure 1. Maximum power factor as a function of the corresponding carrier concentration for the studied compounds in the temperature range from 300 K to 1000 K.

This page shows some statistical data of 361 compounds and 94 promising ones to give you an overall impression about what they are. These compounds are grouped according to their (1) composition, (2) number of atoms in the primitive cell, and (3) crystal system. The statistical data shows that compounds with high power factor tend to have a simple structure: most of the promising candidates are binary or ternary compounds with the number of atoms in a primitive cell less than 20. Moreover, half of the promising compounds have cubic symmetry (47 cubic vs 47

tetra. & ortho.), although the proportion of cubic compounds among all compounds is much smaller (94 cubic vs 267 tetra. & ortho.). It would be convenient to have some simple indexes that help quickly evaluate the thermoelectric performance of a material. For example, average atomic mass, number of atoms in primitive cell. These properties are easily obtained and can be combined with machine learning models to predict more complex properties. So the question is, for thermoelectric properties such as power factor and figure of merit, which simple index is most relevant to their values or at least can be used to group data?

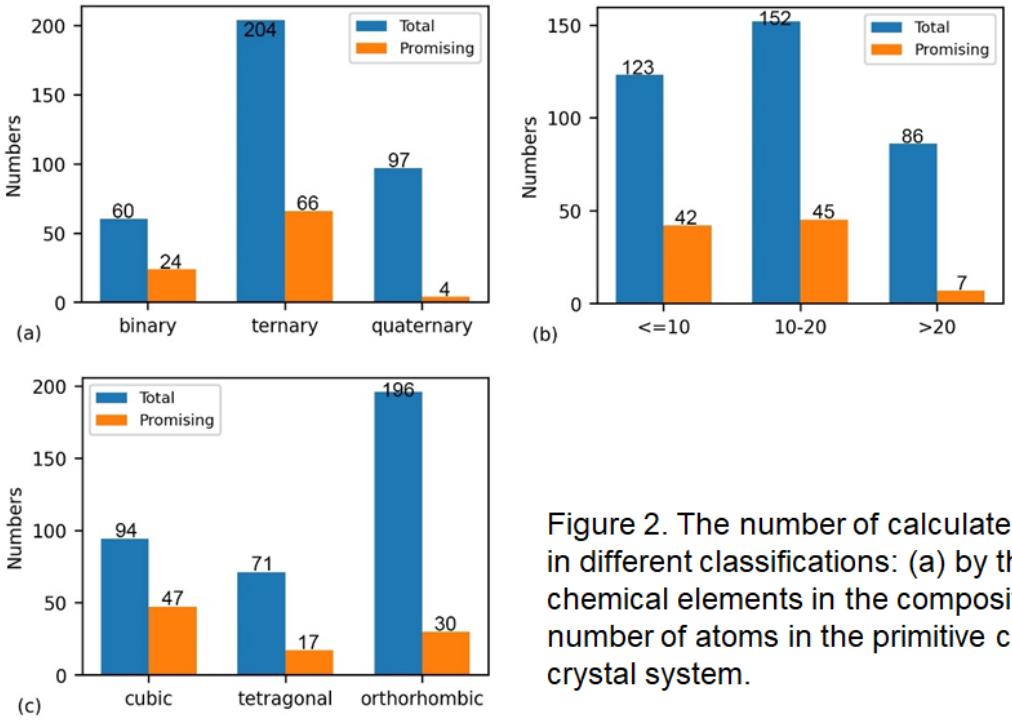

Figure 2. The number of calculated compounds in different classifications: (a) by the number of chemical elements in the composition; (b) by the number of atoms in the primitive cell; (c) by the crystal system.

Let's recall the formulas introduced in methodology, many formulas include conductivity effective mass mc or DOS effective mass md. mobility is inversely proportional to mc, while carrier concentration and seebeck coefficient are proportional to md. Therefore, these two parameters are highly related with final power factor value or figure of merit values. Let's see the results.

m_d^* and m_c^* enter into every formulas related with electronic transport properties

$$\frac{1}{m_c^*} = \frac{1}{3}\left(\frac{1}{m_{\parallel}^*} + 2\frac{1}{m_{\perp}^*}\right)$$

$$m_d^* = N^{2/3}\left(m_{\parallel}^* m_{\perp}^{*2}\right)^{1/3}$$

$$\mu = \frac{e\langle\tau\rangle}{m_c^*}$$

$$n = \frac{\left(2m_{d_0}^* k_B T\right)^{3/2}}{3\pi^2\hbar^3}\int_0^{\infty}\left(-\frac{\partial f}{\partial z}\right)\left(z+\beta z^2\right)^{3/2} dz$$

$$\alpha \approx \frac{2\pi^{2/3}k_B^2 T m_d^*}{3^{5/3} e n^{2/3}\hbar^2}(r+3/2)$$

Here the pictures show the relationship between maximum power factor and md/mc for both types of transport. The increasing trend is clear. I also calculate the Pearson correlation coefficient between these two variables. For n-type, the value is 0.403, while for p-type, it is 0.5857. The Pearson correlation coefficient is not very high, but still verify there is a proportion relationship between these variables.

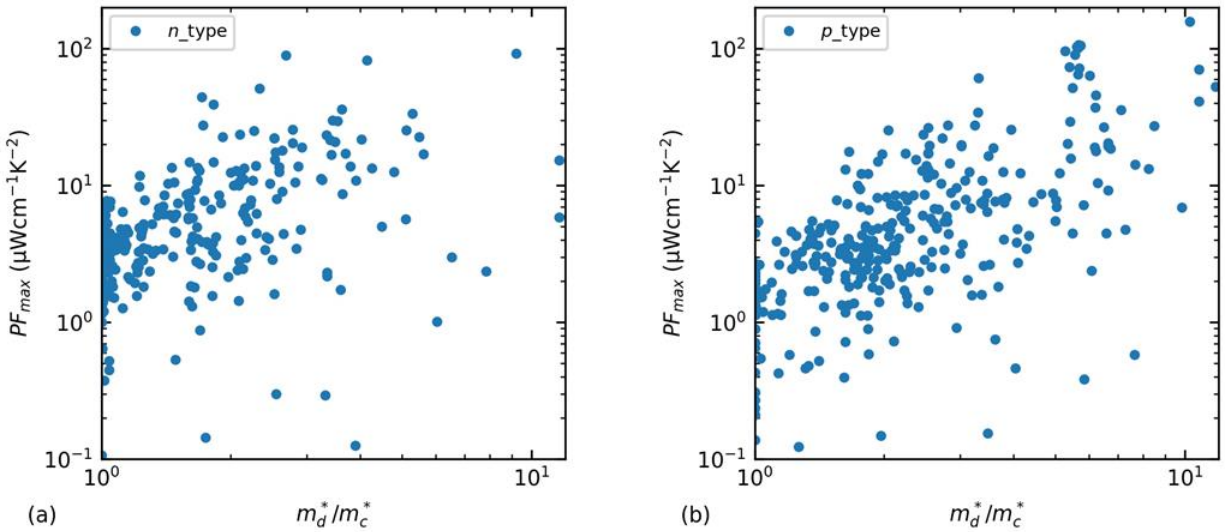

Figure 4. Maximum power factor versus m_d^*/m_c^* for the studied compounds

By adding one more parameter κ_(L,300K) at the denominator. these two pictures show the maximum figure of merit plotted against (m_d^*)/((m_c^* κ_(L,300K))) for the promising compounds. There is also a clear trend that the higher the (m_d^*)/((m_c^* κ_(L,300K))), the higher the maximum figure of merit. The Pearson correlation coefficient for n-type transport is 0.7977, while that is 0.6220

for p-type transport. Although such a correlation coefficient is still a bit low , we believe that using these three parameters or the indexes most related with them as an input in a machine learning model could results in a high-accuracy prediction of the figure of merit.

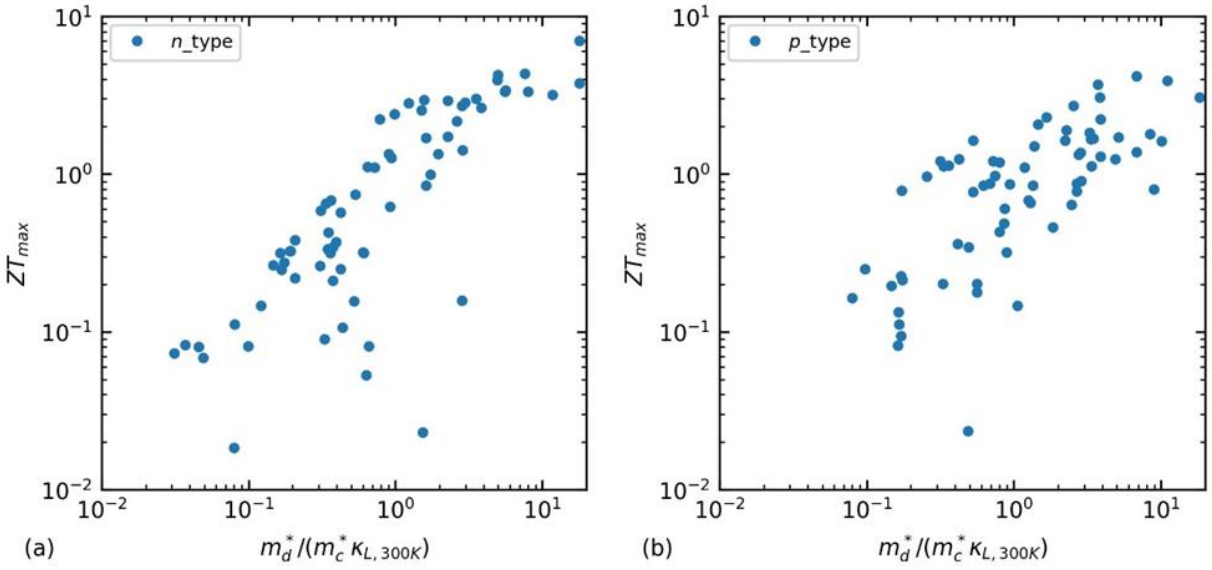

Figure 5. Maximum figure of merit versus $m_d^*/(m_c^* \kappa_{L,300K})$ for the studied compounds

The first I want to introduce is CoAsS like compounds. This group of materials includes 15 compounds. These compounds have cubic structure with space group P213 and they belong to pyrite type structures. Our calculation show that these compounds are very good p-type thermoelectric materials.

$X_4Y_4Z_4$ (X=VIII B; Y=IV A, V A; Z=VI A)

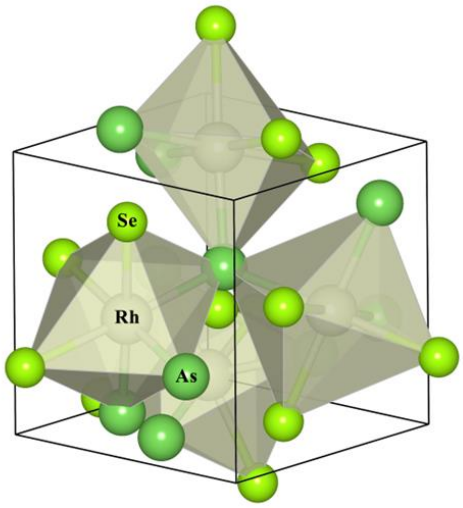

Compounds with this chemical formula, including RhAsSe, RhSbTe, IrSbTe, IrBiSe, IrBiTe, RhBiSe, RhBiTe, CoAsS, CoAsSe, CoPS, CoPSe, RhPSe, CoSbS, PtSnSe, and PtGeTe. These compounds have the same structure (space group $P2_13$) and they belong to the pyrite structure type. They are found to be good p-type thermoelectric materials due to their large power factor.

These graphs show band structures. I use these four compounds as an example. They are all indirect gap semiconductors. Their CBMs are located along several paths. However, their VBMs are located just along the Γ-M path. Well the degeneracy of points along the Γ-M path is large (N=12). It means there are 12 symmetry equivalent carrier pockets in the Brillouin zone, which will give a large DOS effective mass. Besides, the VBMs are dispersive and the corresponding conductivity effective masses are small. Thus, these compounds should have very large DOS effective mass and small conductivity effective.

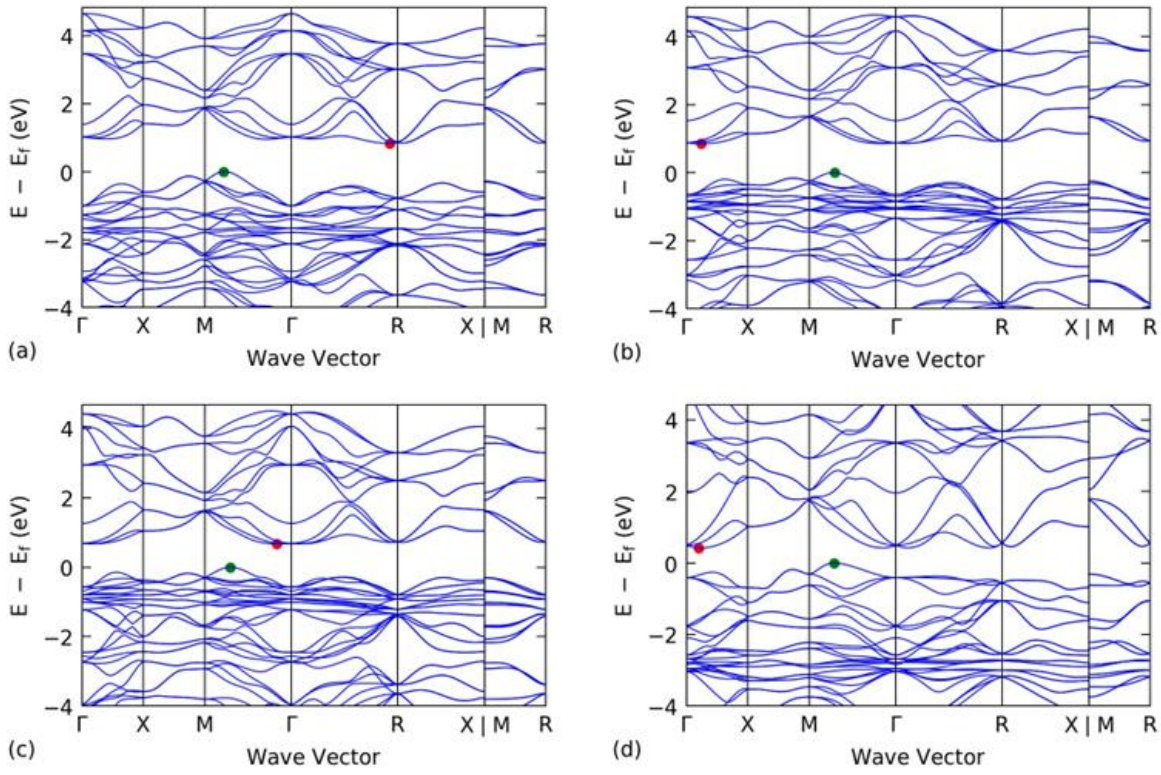

Figure 6. Band structures of (a) RhAsSe, (b) CoAsS, (c) CoAsSe, and (d) PtSnSe

According to the calculation, they truly have large md and small mc for VBM, as this table shows. As discussed in the last section, these compounds are expected to have a high power factor.

Table 1. Key parameters for p-type transport

	m_c^* (m_e)	m_d^* (m_e)	Ξ (eV)	N	E_g (eV)	c (GPa)	ε_∞	ε_0
CoAsS	0.5128	2.8524	13.58	12	0.85	139.60	24.79	31.91
CoAsSe	0.4413	2.4915	12.45	12	0.67	121.86	28.29	36.55
CoPS	0.4862	2.7459	14.49	12	1.14	164.48	21.40	27.02
CoPSe	0.4349	2.4668	13.50	12	0.84	142.05	24.88	31.81
CoSbS	0.5315	2.9145	14.93	12	0.55	105.20	28.54	38.17
RhPSe	0.3805	2.1787	13.94	12	1.11	126.03	19.99	24.02
RhAsSe	0.3712	2.0853	12.97	12	0.83	109.46	22.04	27.08
RhBiSe	0.3545	1.9159	13.25	12	0.13	74.64	34.54	44.90
RhBiTe	0.2798	1.5197	13.67	12	0.07	69.88	41.99	53.79
RhSbTe	0.2929	1.6533	14.66	12	0.37	84.43	28.13	36.32
IrBiSe	0.3601	1.9450	12.94	12	0.38	90.84	25.90	34.50
IrBiTe	0.3152	1.7895	13.33	12	0.33	87.55	28.69	38.23
IrSbTe	0.3045	1.8577	14.20	12	0.70	102.02	20.93	27.82
PtSnSe	0.3206	1.9248	13.67	12	0.42	73.29	27.61	36.34
PtGeTe	0.2307	1.4327	15.46	12	0.17	84.80	33.18	41.78

Their power factors are extremely high in a wide temperature and carrier concentration range. The maximum values of some of them, such as CoAsSe, CoPS, CoPSe, RhPSe, and RhAsSe(Rhodium), could be even higher than 100 mW·cm−1·K−2 according to our calculation. Just a reminder that the power factor values of the state-of-the-art thermoelectric materials, such as Bi2Te3 and PbTe, are usually 30 – 50 mW·cm−1·K−2.

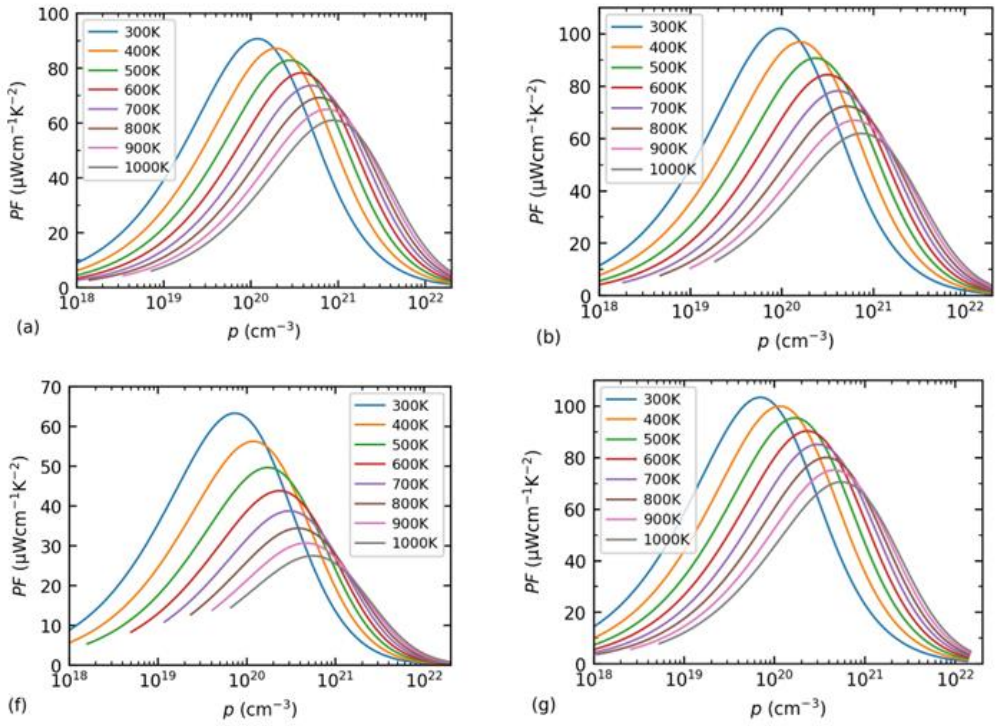

Figure 7. Power factor of (a) CoAsS, (b) CoAsSe, (f) PtSnSe, and (g) RhAsSe.

However, they also have high lattice thermal conductivity, as shown here. Due to this, the figure of the merit of these compounds are not much greater than those state-of-the-art thermoelectric materials. So for this group of materials, the most important way to improve their ZT value is reducing the lattice thermal conductivity. Which can be achieved, for example, by alloying among these compounds.

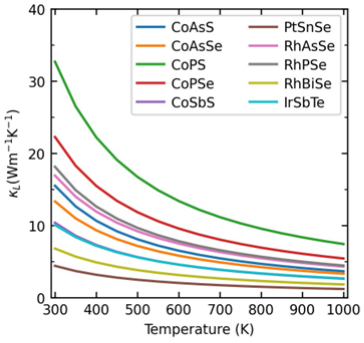

Figure 8. Lattice thermal conductivity

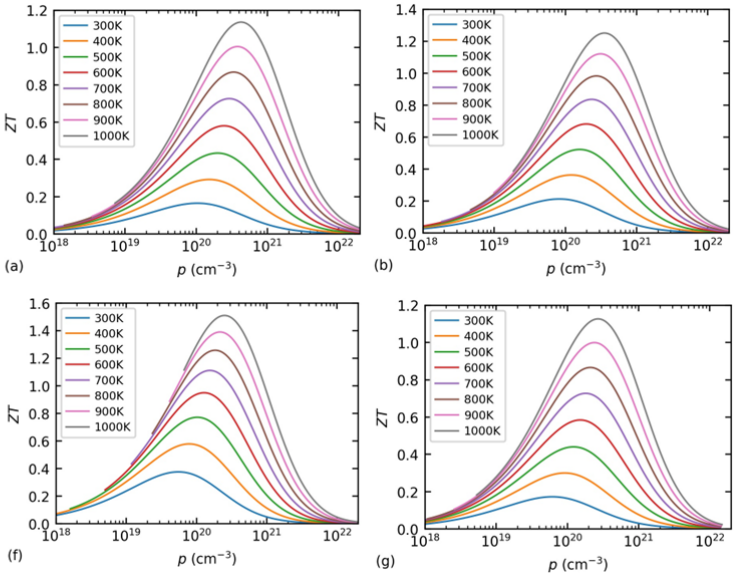

Figure 9. Figure of merit (a) CoAsS, (b) CoAsSe, (f) PtSnSe, and (g) RhAsSe.

CdSe2 is one of the promising n-type thermoelectric materials I found. The unit cell contains 12 atoms (4 Cd and 8 Se) and has a space group Pa-3. It is also a pyrite type structure.

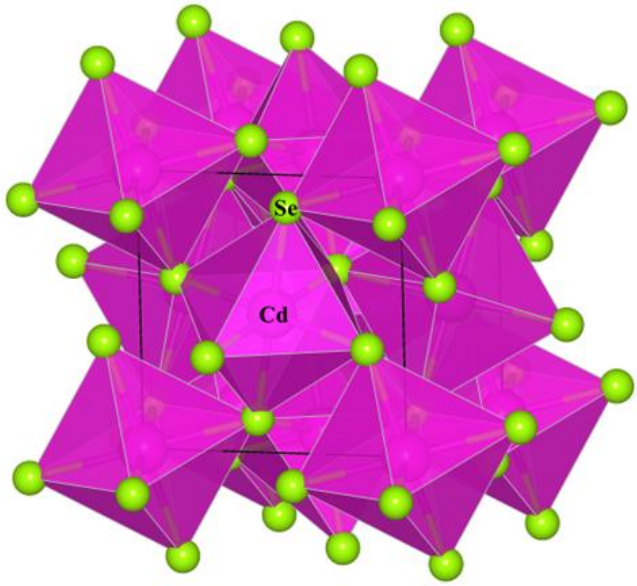

The structure of $CdSe_2$ has a space group *Pa*-3 (pyrite type structure). Cd atoms occupy the corner and each of them forming an octahedron with six Se atoms around. Different octahedrons are connected by one Se atom. This compound is found to be a promising n-type thermoelectric material

According to its band structure, Its VBM is located at the Γ point while CBM is along the Γ-R path. The CBM is dispersive and has a small conductivity effective mass. Meanwhile, the band degeneracy N of CBM is 8. Thus its has a large md/mc value.

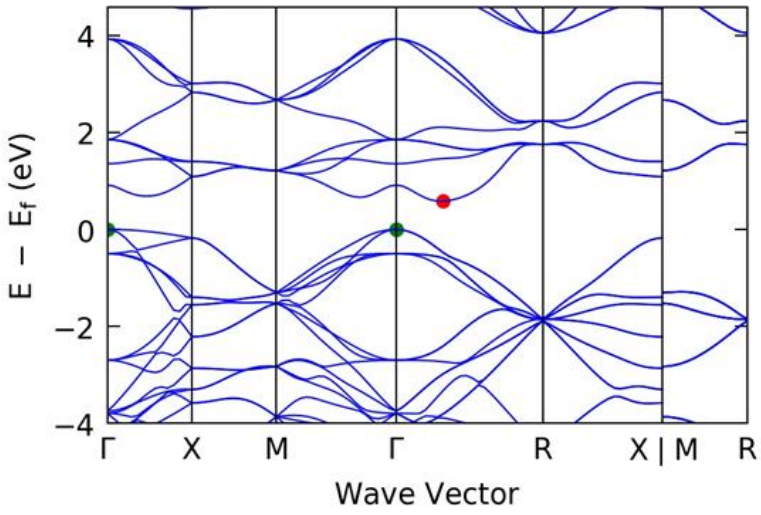

Figure 10. Band structures of $CdSe_2$

Table 2. Key parameters for n-type transport

	m_c^* (m_e)	m_d^* (m_e)	Ξ (eV)	N	E_g (eV)	c (GPa)	ε_∞	ε_0
$CdSe_2$	0.41	1.64	10.19	8	0.58	23.96	11.41	19.90

Here shows transport properties of CdSe2. The power factor value is relatively high, what's more important is it has a very low lattice thermal conductivity. Thus. The ZT value could exceed 1.

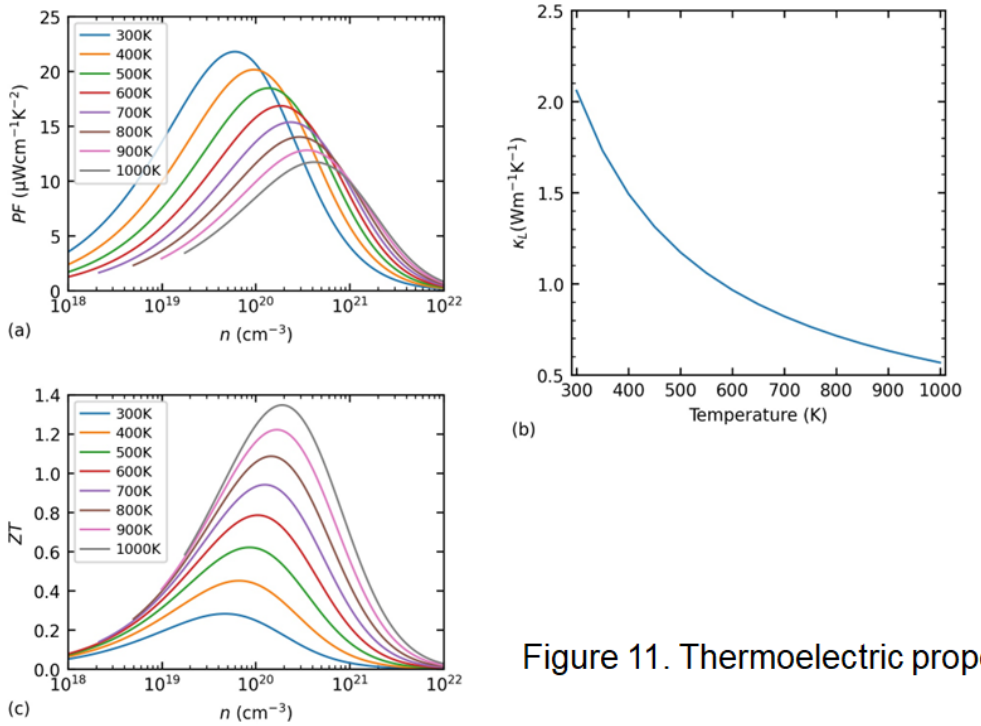

Figure 11. Thermoelectric properties of $CdSe_2$.

The above are cubic compounds. Next I will introduce some orthorhombic compounds. The most interesting ones are SnSe-like compounds. SnSe single crystal is a well known thermoelectric material with the record high figure of merit around 2.6 in 900 K. Its polycrystal and solid solutions are also reported to have high ZT values. Thus, It is natural to think that those compounds, which are composed of elements near Sn and Se in the periodic table and adopt the similar crystal structure, should also have good thermoelectric performance. Luckily, structures extracted from MP include such compounds. SnSe has two phases, the low temperature alpha-phase with space group Pnma and high temperature beta-phase with space group Cmcm. Compounds similar with alpha-phase include five ones, The unit cell contains eight atoms (four IVA atoms, four VIA atoms) and adopts double layer structure. In each layer, atoms are connected in a distorted zig-zag structure. The adjacent layers along the c-axis are weakly bonded by a combination of van der Waals forces and electrostatic attractions.

Pnma-type

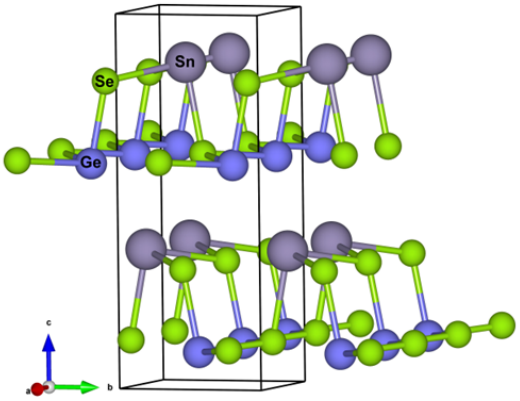

Compounds belong to this group include $Sn_2Ge_2Se_4$, $Ge_4Se_2S_2$, Ge_4Se_4, $Sn_2Pb_2S_4$, Ge_4Te_4. . The unit cell contains eight atoms (four IVA atoms, four VIA atoms). The IVA and VIA atoms are combined with strong heteropolar bonds to form the crystalline layers. The adjacent layers along *c*-axis are weakly bonded by a combination of van der Waals forces and electrostatic attractions.

The band structures of these compounds are shown here. Similar to that of SnSe, they are in-direct gap semiconductors and there are multiple band valleys near the gap for both conduction band and valence band. These band extrema usually are highly anisotropic. Moreover, since they are orthorhombic structures, the band degeneracy of these band valleys are small, usually equals to 2.

Pnma-type

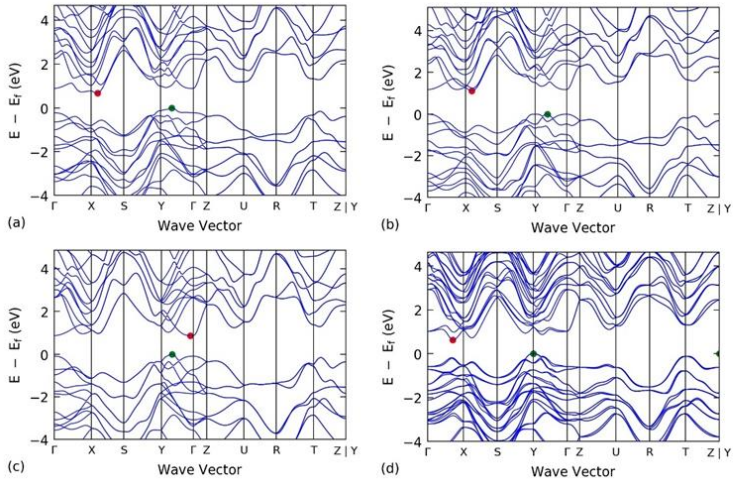

Figure 12. Band structures of (a) $Sn_2Ge_2Se_4$, (b) $Ge_4Se_2S_2$, (c) Ge_4Se_4 and (d) $Sn_2Pb_2S_4$.

Our calculation shows this group of compounds are better to be n-type thermoelectric materials than p-type. Their n-type power factor could be larger than 10. The exception is Ge4Te4, both n-type and p-type's power factor could be larger than 10. You see, compared with the power factor of cubic compounds shown above, such a power factor value is not high enough. However,These compounds have extremely low lattice thermal conductivity. Except Ge4Te4, the lattice thermal conductivities at 300 K of these compounds are already lower than 0.5 W·m−1·K−1, close to the amorphous limit. Such a low lattice thermal conductivity is mainly due to their large grüneisen coefficients, thus indicating strong anharmonicity intrinsically in these compounds.

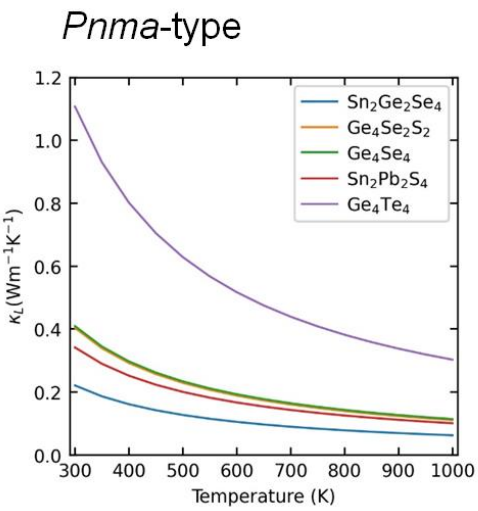

Table 3. Phonon velocity v and Grüneisen parameter γ

	v_{TA}	$v_{TA'}$	v_{LA}	γ_{TA}	$\gamma_{TA'}$	γ_{LA}
$Sn_2Ge_2Se_4$	1552.21	2333.82	3085.96	5.23	3.97	3.75
$Ge_4Se_2S_2$	2478.90	2024.00	3231.27	5.17	3.39	3.01
Ge_4Se_4	3618.81	1646.25	3019.41	5.08	4.01	2.48
$Sn_2Pb_2S_4$	1453.16	2057.29	2863.01	4.66	2.87	2.76
Ge_4Te_4	1718.25	2694.27	3481.99	3.64	2.78	2.39

Due to such low lattice thermal conductivity, their figure of merit values could be larger than 1 in a wide range of temperatures and carrier concentrations.

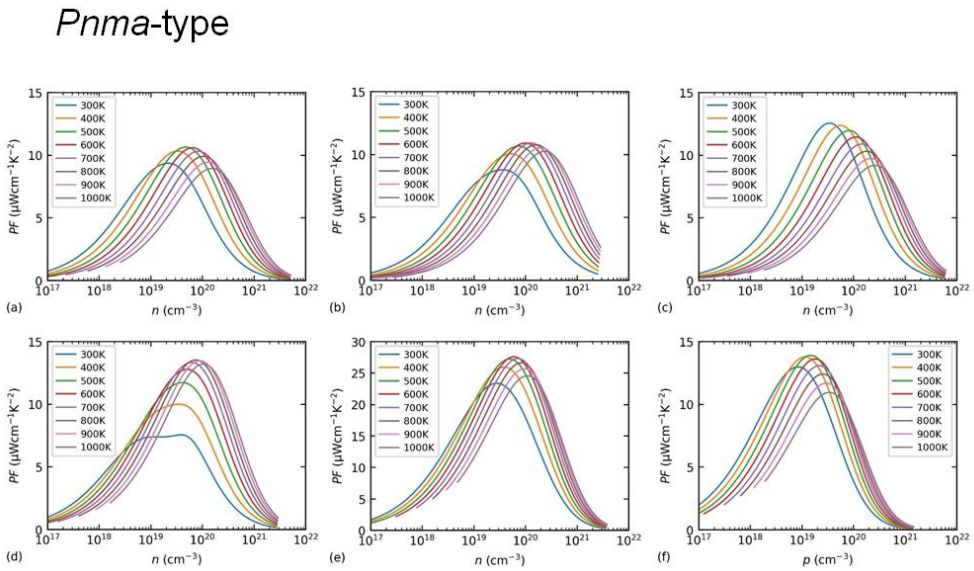

Figure 13. Power factor of (a) $Sn_2Ge_2Se_4$, (b) $Ge_4Se_2S_2$, (c) Ge_4Se_4, (d) $Sn_2Pb_2S_4$, (e)(f) Ge_4Te_4.

Compounds similar with beta-phase include PbSe and PbS, The unit cell also contains eight atoms (four IVA atoms, four VIA atoms) and adopts double layer structure. In each layer, atoms are connected in a less distorted structure. Between the layers are weak Van der Waals bonding.

Cmcm-type

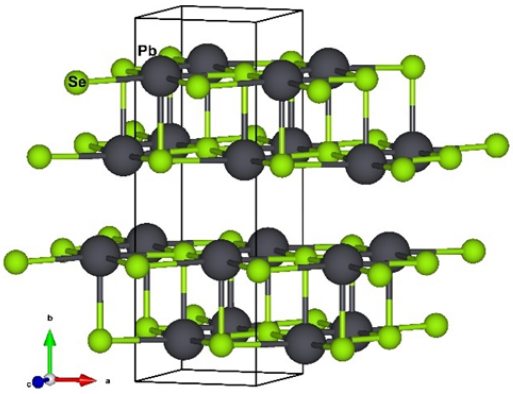

Compounds belong to this group include Pb_4Se_4, Pb_4S_4. The unit cell contains eight atoms and adopts a double-layered structure. Different from the α-phase structure, within each layer of β-phase, one IVA (or VIA) atom is instead bonded to five neighboring VIA (or IVA) atoms in a less distorted structure. The adjacent layers along *b*-axis are weakly bonded by a combination of van der Waals forces and electrostatic attractions.

This page shows their band structures. Same as beta-phase SnSe, they are direct gap semiconductors with band extrema along T-Y path (N=2). There are multiple band valleys for both conduction band and valence band near the band gap.

Cmcm-type

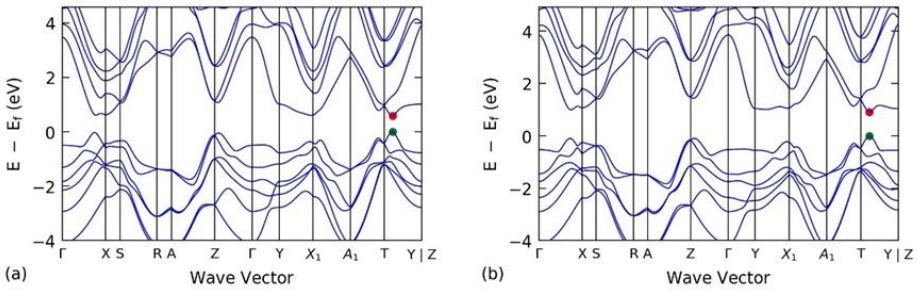

Figure 16. Band structures of (a) Pb_4Se_4, (b) Pb_4S_4.

For these two compounds, both n-type and p-type power factor are high,

Cmcm-type

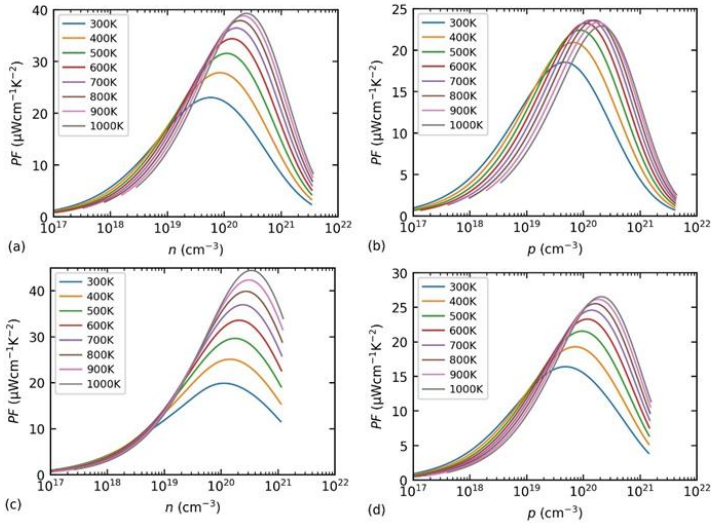

Figure 17. Power factor of (a)(b) Pb_4Se_4, (c)(d) Pb_4S_4.

The lattice thermal conductivity, not as low as alpha phase, but still is very low, due to their low phonon velocity and strong anharmonicity in the lattice.

Cmcm-type

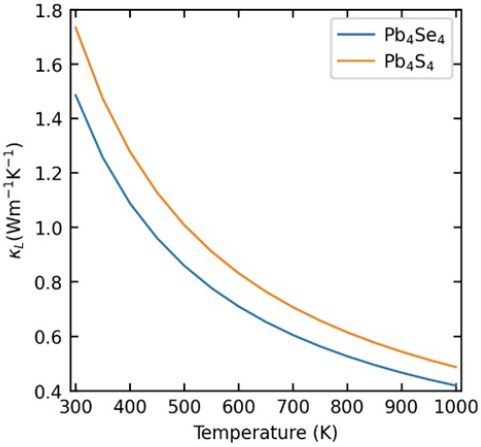

Figure 18. Lattice thermal conductivity

Table 4 Phonon velocity v and Grüneisen parameter γ

	v_{TA}	$v_{TA'}$	v_{LA}	γ_{TA}	$\gamma_{TA'}$	γ_{LA}
Pb_4Se_4	1045.73	1986.53	2537.70	4.85	2.26	1.34
Pb_4S_4	896.77	1909.94	2736.21	6.89	2.91	1.79

Therefore, their figure of merit values could be higher than 1 in a wide range of temperature and carrier concentration. And these compounds are excellent n-type and p-type thermoelectric materials.

Cmcm-type

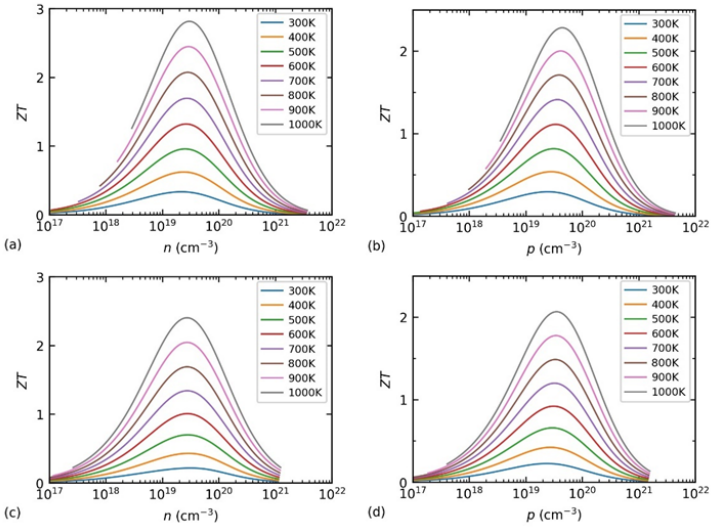

Figure 19. Figure of merit of (a)(b) Pb_4Se_4, (c)(d) Pb_4S_4.

Reading:

[1] Tao Fan, Artem R. Oganov. "AICON: A program for calculating thermal conductivity quickly and accurately." *Computer Physics Communications* 251 (2020): 107074.

[2] Tao Fan, Artem R. Oganov. "AICON2: A program for calculating transport properties quickly and accurately." *Computer Physics Communications* 266 (2021): 108027.

[3] Tao Fan, Artem R. Oganov. "Discovery of high performance thermoelectric chalcogenides through first-principles high-throughput screening." *Journal of Materials Chemistry C* 9.38 (2021): 13226–13235.